

# Computational subunits in thin dendrites of pyramidal cells

Alon Polsky<sup>1</sup>, Bartlett W Mel<sup>2</sup> & Jackie Schiller<sup>1</sup>

The thin basal and oblique dendrites of cortical pyramidal neurons receive most of the synaptic inputs from other cells, but their integrative properties remain uncertain. Previous studies have most often reported global linear or sublinear summation. An alternative view, supported by biophysical modeling studies, holds that thin dendrites provide a layer of independent computational 'subunits' that sigmoidally modulate their inputs prior to global summation. To distinguish these possibilities, we combined confocal imaging and dual-site focal synaptic stimulation of identified thin dendrites in rat neocortical pyramidal neurons. We found that nearby inputs on the same branch summed sigmoidally, whereas widely separated inputs or inputs to different branches summed linearly. This strong spatial compartmentalization effect is incompatible with a global summation rule and provides the first experimental support for a two-layer 'neural network' model of pyramidal neuron thin-branch integration. Our findings could have important implications for the computing and memory-related functions of cortical tissue.

It is well established that dendrites of pyramidal neurons contain many types of voltage-dependent channels and can generate isolated dendritic spikes<sup>1–7</sup>, although direct evidence regarding the rules of synaptic integration in these cells remains partial and conflicting<sup>8–15</sup>. Neurophysiological studies of pyramidal neurons have often focused on interactions between the axosomatic and distal calcium spike initiation zones, and the influences of synaptic input thereupon<sup>13,15,16–20</sup>. Other studies have suggested that active dendritic conductances, in conjunction with synaptic scaling, exist to counteract passive synaptic sublinearities and distance-dependent filtering of synaptic currents, thereby leading to a simpler, more linear-behaving cell<sup>10,11,21–24</sup>. In contrast, relatively few experiments have systematically examined the 'arithmetic' of synaptic summation in pyramidal neurons, and fewer still have focused on summation within and between thin basal and apical oblique dendrites<sup>3,9,10,15</sup>, where most excitatory synapses actually lie<sup>25–27</sup>. The goal of the present study was to address this shortcoming, using hypothesis-driven experiments to distinguish between two different models of excitatory synaptic integration in thin dendrites of pyramidal neurons.

The global summation model in its simplest (linear) form holds that the combined subthreshold effects of two or more excitatory synapses can be determined by summing their individual responses, without regard to their absolute or relative locations in the dendritic tree. The global model can also accommodate a single output nonlinearity. If the output nonlinearity is compressive, such as a logarithmic function, the response to two or more inputs is always less than the sum of the individual responses and summation is called sublinear. If the output nonlinearity is expansive, such as a quadratic or exponential function, the combined response always exceeds the linear prediction and summation is called superlinear. Other output nonlinearities

are possible, such as the S-shaped sigmoidal nonlinearity that crops up in many physical and neural systems; in this case, summation would be expected to range from the superlinear to the sublinear depending on stimulus intensity.

Studies that have directly examined excitatory synaptic integration involving the thin branches of pyramidal neurons have most often reported overall linear or sublinear summation in both apical and basal dendritic trees<sup>9–11,15</sup>. The absence of superlinear summation in these studies is notable, given that pyramidal neuron thin branches can respond to focal synaptic stimulation with regenerative NMDA, sodium, and/or calcium spikes that remain confined within the stimulated branch<sup>28–30</sup>. A local spike-generating mechanism should in principle lead to superlinear summation whenever two or more sub-threshold inputs are sufficiently concentrated in space, and prolonged in time, that together they trigger a local dendritic spike. In a rare example of this, clear cases of superlinear summation were observed for two spatially segregated inputs delivered to the apical tree of a layer-5 pyramidal neuron<sup>12</sup>. However, given that these experiments were carried out in the presence of an NMDA channel blocker, which should suppress or eliminate synaptically evoked spikes within the thin branches themselves<sup>28</sup>, the observed superlinearity was most likely mediated by voltage-dependent boosting from the calcium spike initiation zone in the apical tuft<sup>16–18,20</sup>. Thus, existing data are consistent overall with the view that excitatory summation in thin dendrites of pyramidal neurons obeys a global linear or sublinear summation rule, unless the calcium spike-generating mechanism in the apical tuft becomes involved, in which case summation can be superlinear. The question as to whether active currents in thin branches might also contribute to superlinear summation has yet to be clearly resolved.

<sup>1</sup>Department of Physiology, Technion Medical School, Bat-Galim, Haifa 31096, Israel. <sup>2</sup>Department of Biomedical Engineering University of Southern California, University Park, Los Angeles, California 90089-1451, USA. Correspondence should be addressed to J.S. (jackie@tx.technion.ac.il).

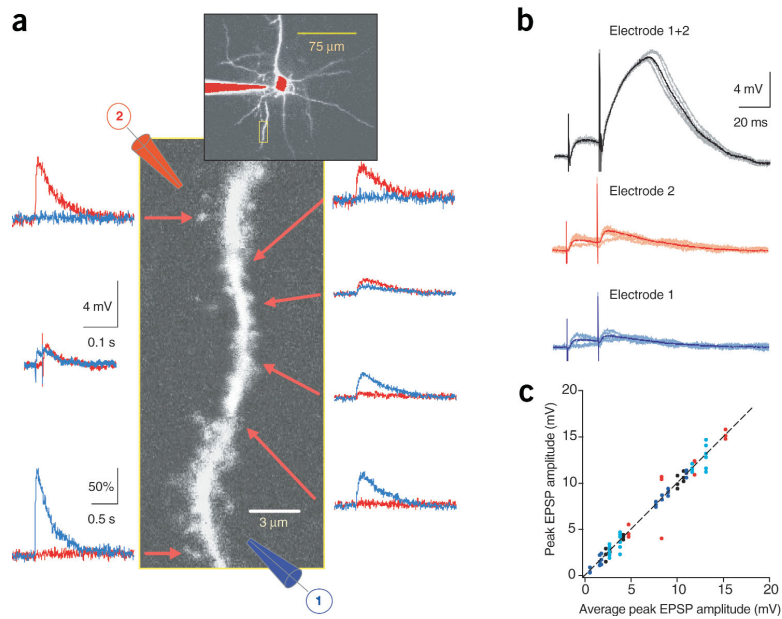


**Figure 1** Focal extracellular synaptic stimulation of identified regions in fine basal dendrites. **(a)** A layer-5 pyramidal neuron was loaded with calcium sensitive dye OGB-1 (200 μM) using the somatic patch electrode (upper panel). A dendritic branch was visualized (yellow box, lower panel) using a confocal microscope, and two theta electrodes were positioned in close proximity to the selected branch (shown schematically in red and blue). Somatic voltage responses and concomitant dendritic calcium transients were measured at different dendritic loci (indicated by red arrows) during separate stimulation of the two electrodes. Traces are color coded to indicate which electrode was stimulated. Calcium transients peaked in spines near the stimulating electrodes and gradually decayed to baseline along the dendritic segment. **(b)** Five consecutive somatic voltage traces evoked by a constant stimulus at each electrode separately (Electrode 1, Electrode 2) and together (Electrode 1+2). The average voltage trace in each condition is shown by a darker line. **(c)** The variability of peak voltage responses, presented as the measured peak EPSP of each separate trial versus the average peak at a range of stimulus intensities in four different neurons (indicated by different colors).

An alternative to the global model for synaptic integration in pyramidal neurons has been proposed that involves two layers of processing<sup>31,32</sup>, based in part on the observation that dendritic spikes evoked by focal synaptic stimulation remain confined within a single thin branch<sup>28–30</sup>. The two-layer model holds that pyramidal cells first process their synaptic inputs within separate thin-dendrite compartments or subunits, each of which is governed by its own sigmoidal thresholding nonlinearity. In a second stage of processing, the subunit outputs are combined linearly to determine the overall response of the cell. Interestingly, if a global output nonlinearity is included to represent the axosomatic spiking mechanism of the cell, this abstract formulation for the pyramidal neuron's input-output behavior is the same as that used to describe a conventional two-layer artificial neural network with sigmoidal hidden units<sup>33</sup>.

A key prediction of the two-layer model, but not of the global summation model, is that summation should obey different rules for inputs delivered to the same versus different thin branches of the cell<sup>31</sup>. In particular, within-compartment summation should be modulated by an S-shaped nonlinearity that gives rise to linear, superlinear or sublinear summation depending on stimulus strength and balance. In contrast, between-compartment summation should always be linear.

## RESULTS

### Focal activation of specific dendritic segments

To distinguish between the global and two-layer models of synaptic integration, we performed whole-cell recordings from layer-5 pyramidal neurons and focally activated synaptic inputs innervating different dendritic sites. Fine basal and oblique dendrites of layer-5 pyramidal neurons were visualized with confocal fluorescence imaging. The locations of activated synapses were determined for each experiment using calcium imaging, which showed small localized transients in the internal calcium concentration ( $[Ca^{2+}]_i$ ) in dendritic segments that were 3–8 μm long and selective activation of dendritic spines in close proximity to the stimulating electrodes (Fig. 1a).

Addition of the NMDA receptor blocker APV, as well as the AMPA receptor blocker CNQX, completely blocked the excitatory synaptic response and the concomitant calcium transient, ruling out the possibility of direct dendritic activation ( $n = 6$ ; data not shown). Synaptic responses showed variability, including failures, but the variability from trial to trial was nearly always small compared with the mean response (Fig. 1b,c).

### Comparison of within-branch and between-branch summation

The basic experimental approach was to focally activate two dendritic sites, first individually and then simultaneously, on the same or on different dendritic branches. We then compared the somatic response to the combined stimulus (the combined response) to the arithmetic sum of the two individual somatic responses<sup>9,10,14,31</sup> (Fig. 2). The stimulus at each location usually consisted of a pair of pulses separated by 20 ms (comparisons with single-pulse stimuli are shown in Fig. 4). We could not exclude the possibility that in addition to synapses activated at the sites of focal stimulation, other synapses were activated elsewhere in the dendritic arbor by itinerant axons passing near the stimulating electrodes. However, we rarely if ever observed calcium signals elsewhere in the basal dendrites, which would have suggested that this type of rogue activation was occurring. If it did occur, its random nature would tend to lead to an underestimate of the main effects of spatial integration reported here, as these depend critically on spatially structured input.

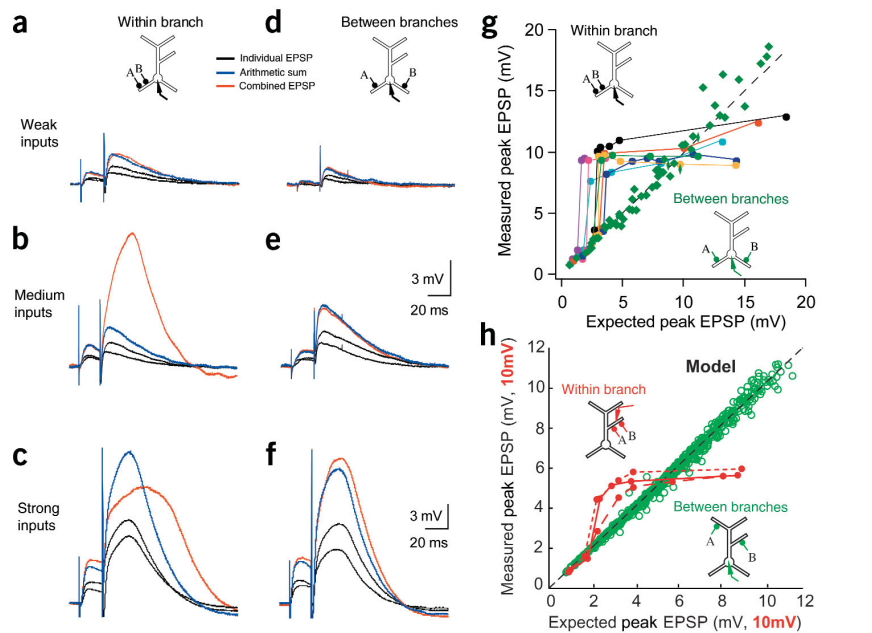
Summation of inputs activating nearby sites on the same dendritic branch depended on the amplitude of the individual excitatory postsynaptic potentials (EPSP). Small EPSPs summed linearly (Fig. 2a). Above a threshold value, however, EPSPs summed superlinearly, that is, the combined response was significantly larger than the arithmetic sum of the two individual responses (Fig. 2b). We defined the threshold voltage for superlinear summation as the somatic potential at which the combined response exceeded the linear prediction by 25% or more. The average threshold for two inputs activating the same basal branch was  $3.3 \pm 0.9$  mV, measured at the soma ( $n = 20$ ; 1 μM of

**Figure 2** Comparison of within-branch and between-branch summation. Two stimulating electrodes were positioned near selected basal dendrites of a layer-5 pyramidal neuron.

Electrodes were activated first individually (black traces) and then simultaneously (red traces), and somatic EPSPs were recorded. Blue traces show the arithmetic sum of the two individual responses. Voltage traces are averages of four individual sweeps. (a–c) Within-branch summation. The two electrodes were positioned near the same dendritic branch, separated by 20  $\mu\text{m}$  (150  $\mu\text{m}$  from the soma). Summation was (a) linear for weak stimuli, (b) strongly superlinear for intermediate stimuli and (c) slightly sublinear for strong stimuli.

(d–f) Between-branch summation. The two electrodes stimulated different branches. Summation was linear for (d) weak or (e) intermediate stimuli, with a slight superlinearity at (f) higher stimulus intensities.

(g) Summary plot shows predicted versus actual combined responses in seven basal dendrites and one apical oblique dendrite (pink curve). Colored circles show sigmoidal modulation of within-branch summation (blue and yellow, without BCC; dark green trace, with locally applied 10  $\mu\text{M}$  BCC; five remaining traces, 1  $\mu\text{M}$  BCC). Dashed line denotes exact linear summation. Green diamonds show between-branch summation experiments (12 branch pairs, 4 of them apical oblique dendrites). (h) Modeling data: summation of single-pulse EPSPs in the apical oblique dendrites of a CA1 pyramidal cell model showed a similar overall pattern<sup>31</sup>, including sigmoidally modulated within-branch summation (red circles) and linear between-branch summation (open green circles). Within-branch data are for dendrites attached to the apical trunk 92  $\mu\text{m}$  (short dashes), 232  $\mu\text{m}$  (solid) and 301  $\mu\text{m}$  (long dashes) from the soma. Because of the uneven distances to the somatic recording electrode, recordings shown were made within the respective dendrite; for these data, axis values are scaled up  $\times 10$ , thus 0 mV, 20 mV, 40 mV, and so on.



the GABA<sub>A</sub> receptor blocker Bicuculline methiodide (BCC) was added to the extracellular solution; interelectrode distance was 20–40  $\mu\text{m}$ ; distance from soma of proximal electrode was 80–250  $\mu\text{m}$ . At that threshold voltage, the peak of the summed EPSPs was  $262 \pm 101\%$  larger than the linear prediction on average (well above the 125% threshold criterion). The threshold and amplification of the summed potential did not significantly change when inhibition was left intact (no BCC was added to the bath) or when inhibitory transmission was completely blocked (10–20  $\mu\text{M}$  BCC was applied focally in the neighborhood of the activated dendrite). The average thresholds were  $3.6 \pm 0.6$  mV and  $3.7 \pm 0.9$  mV, and the peaks of the

summed EPSPs at threshold were  $246 \pm 49\%$  and  $248 \pm 31\%$  larger than the linear prediction when no BCC and 10–20  $\mu\text{M}$  BCC were present in the bath, respectively ( $n = 7$  with no BCC,  $n = 4$  with 10–20  $\mu\text{M}$  BCC;  $P > 0.05$  as compared with 1  $\mu\text{M}$  BCC). When stimulus intensity at the individual electrodes was further increased, summation of EPSPs gradually became sublinear (Fig. 2c). In most cases when within-branch integration was sublinear, local spikes had been initiated at one or both of the individual stimulus sites, which may in turn have led to a saturation of the ability of the branch to deliver current to the cell body (Fig. 2g). Local spike initiation was identified by the clear thresholding in the stimulus intensity versus response

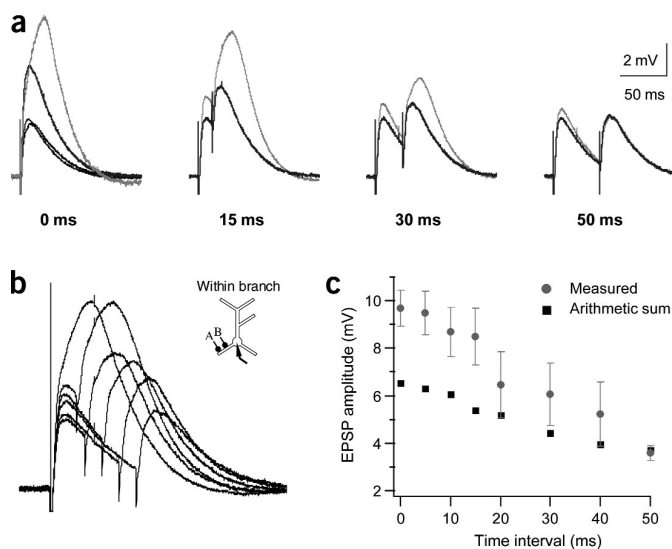


**Figure 3** Time window for superlinear summation of two closely spaced dendritic sites (within-branch summation). (a) Two closely spaced dendritic sites were summed at various time delays (0–50 ms). Measured EPSP (gray) and arithmetic sum (black) of individual EPSPs (lower-amplitude black traces in first frame) are shown for four different time delays. Each trace is an average of ten consecutive responses. Decrease in the amplitude of the combined response is primarily due to the decrease in probability of local spike initiation. (b) Summed responses at various time delays are shown superimposed for comparison. (c) Peak amplitude of the summed response is presented as a function of time delay between activation of the two electrodes. Circles show actual measured peak responses (mean  $\pm$  s.d.); squares show peak of (expected) arithmetic sum. Superlinear summation persists at intervals up to 40 ms.

**Figure 4** The effect of the NMDA receptor blocker APV on within-branch summation for single- and paired-pulse stimulation. A layer-5 pyramidal neuron was stimulated by two electrodes (30  $\mu\text{m}$  apart) on a single branch. (a,b) The voltage responses at the soma (a) for a single pulse and (b) for two pulses at 50 Hz before and after the application of APV (50  $\mu\text{M}$ ) are shown (color scheme for traces as in Fig. 2). The voltage traces are averages of four individual sweeps. (c) Expected versus actual peak somatic voltage responses are plotted for different stimulus intensities. Summation nonlinearity is enhanced for paired pulses at 50 Hz (black) as compared with single-pulse stimuli (red) as evidenced by a much lower, sharper threshold for superlinear summation. (d) Expected versus actual somatic responses are shown at several stimulus intensities for paired-pulse stimuli before (black) and after (blue) application of APV. Linearized summation indicates a prominent role for NMDA currents.

curve, and by the shape of the somatic voltage response<sup>28</sup>. A similar pattern of within-branch summation was observed in apical oblique dendrites as well, including linear, superlinear and sublinear regimes ( $n = 4$ ; Fig. 2g, pink circles).

In contrast to within-branch summation, the rules governing summation of inputs innervating two different basal dendrites were significantly and consistently different. In the between-branch case, summation was essentially linear over a wide range of EPSP amplitudes (Fig. 2d,e). For very large EPSPs, which generally involved local dendritic spikes, slight superlinear integration of the two inputs was sometimes observed (Fig. 2f). Similar results were obtained in 14 experiments from 13 different neurons (Fig. 2g). When inputs were delivered to one basal and one apical oblique dendrite, EPSP summation at the cell body was found to follow a very similar pattern to that shown in Figure 2 ( $n = 4$ ).

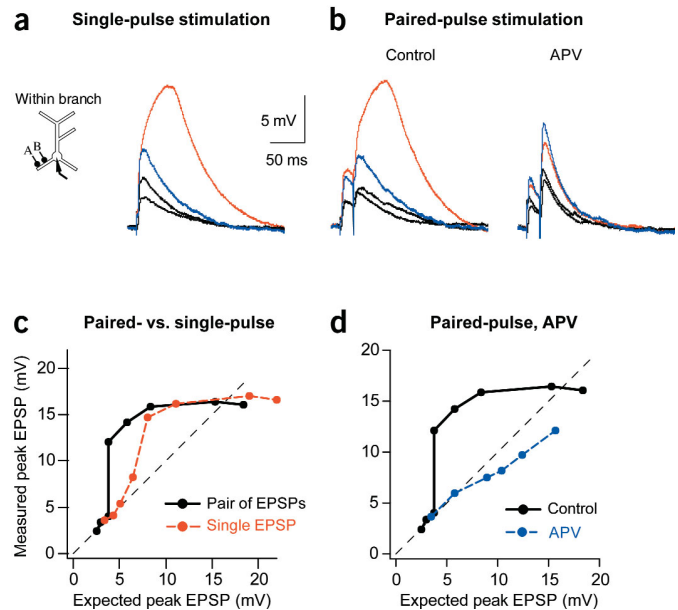
For comparison, Figure 2h shows modeling results of within- versus between-branch summation in the apical oblique dendrites of a previously developed CA1 pyramidal cell model<sup>31,32</sup>. The similar pattern of results seen in a model developed prior to the current experiments, for a different type of pyramidal cell, supports the idea that sigmoidal within-branch summation with linear between-branch summation is a pattern that holds for the thin branches of pyramidal neurons in general.

### The time window for within-branch interactions

The requisite time window for nonlinear summation of two inputs to the same branch was examined using different interstimulus intervals (ISIs). Superlinear within-branch summation could be obtained when the ISIs were 0–40 ms, whereas with longer ISIs the EPSPs summed linearly (Fig. 3). The amplitude of the superlinear amplification decreased as the ISI increased, especially beyond 15–25 ms. Similar results were obtained in four neurons. It is noteworthy that this time window is longer than that described in apical dendrites of the same neuron<sup>20</sup> and in basal dendrites of CA1 neurons<sup>30</sup>.

### Nonlinear summation is NMDA-receptor dependent

The striking difference between within-branch and between-branch summation (Fig. 2g) held for both single-pulse and paired-pulse (50 Hz) stimulation. Quantitatively, however, the superlinear amplification was stronger and the threshold lower for paired-pulse as compared with single-pulse stimuli (Fig. 4a–c; note that pairs were used in Fig. 2). Thus, the threshold needed to evoke superlinear within-branch summation was only  $3.3 \pm 0.6$  mV for paired pulses ( $n = 20$ ; 1  $\mu\text{M}$  BCC) as compared with  $5.3 \pm 1.7$  mV for single pulses ( $n = 9$ ;  $P < 0.01$ ). At the threshold voltage, amplification of paired-pulse stimuli was  $263 \pm 104\%$  as compared with  $185 \pm 60\%$  for single pulses.



Superlinear within-branch summation was dependent on activation of NMDA receptor channels. Addition of 100  $\mu\text{M}$  extracellular APV or 20  $\mu\text{M}$  MK-801, another NMDA receptor antagonist, converted within-branch summation to a linear or sublinear process in seven out of ten neurons (Fig. 4b,d; data for MK-801 not shown). In these neurons, sublinear integration of AMPA-mediated EPSPs was observed for larger EPSPs, whereas smaller EPSPs summed linearly (Fig. 4d)<sup>10,31</sup>. In the remaining three neurons, superlinear within-branch summation was only partially abolished ( $80 \pm 12\%$  reduction) by APV and MK-801 and was unaffected by consecutive addition of the L-type calcium channel blocker nifedipine (10  $\mu\text{M}$ ; 2 out of the 3 neurons; data not shown). Moreover, in these neurons, superlinear amplification in the presence of APV or MK-801 was associated with the appearance of a narrow spike-like component that did not evoke a measurable  $[\text{Ca}^{2+}]_i$  transient (data not shown). This indicates that superlinear integration in these cases might be mediated in part by dendritic voltage-gated sodium channels<sup>30</sup>. The fact that APV eliminated the superlinear within-branch amplification in most neurons, and markedly reduced it in the remaining cases, ruled out the possibility that the superlinear summation was caused by recruitment of additional axons during coactivation of the two stimulating electrodes.

### Size of the within-branch integration compartment

Our finding of sigmoidal within-branch summation and linear between-branch summation bears out the major prediction of the two-layer model of pyramidal cell integration (compare Fig. 2g,h). Some differences were found, however. For simplicity, recent modeling experiments assumed that the long unbranched terminal dendrites were the monolithic integrative subunits of the pyramidal neurons<sup>31,32</sup>. Consequently, these simulation experiments did not explore the effects of intracompartamental space for synaptic integration. Given that basal and oblique dendrites are often hundreds of microns in length, however, it is possible that each branch is actually composed of multiple integrative compartments. To measure the size of an integrative compartment in the basal tree, we varied the distance between the two stimulating electrodes along the same branch (Fig. 5a–d). We found that strong nonlinear interactions occurred only when two conditions were met. First, the stimulating electrodes

activated sites within the same branchlet, that is, the interelectrode dendritic segment did not include a branch point. Second, the distance between the two activated segments was less than 40  $\mu\text{m}$  (Fig. 5b,c). In contrast, when the distance between the two activated sites grew larger than 80  $\mu\text{m}$ , summation of the two EPSPs became essentially linear (Fig. 5a–d;  $n = 6$ ). For intermediate cases, with interelectrode distances of 45–80  $\mu\text{m}$ , two inputs could combine superlinearly (Fig. 5a–d). The amplification was much smaller, however, than that seen for input separations of less than 40  $\mu\text{m}$  and occurred at higher voltage values. On average, superlinear summation in these cells was observed when the combined response exceeded  $6.9 \pm 2.4$  mV, at which point the measured EPSP was  $1.28 \pm 0.16$  times greater than the linear prediction ( $n = 7$ ). As before, addition of APV eliminated these superlinear interactions and turned summation into a linear or sublinear process ( $n = 2$ ; data not shown).

We also examined the summation of inputs delivered to different branchlets, that is, to two dendritic segments separated by a single branch point (Fig. 5e–g; interelectrode distances were 30–50  $\mu\text{m}$  of dendritic length). Overall, the pattern of summation for inputs delivered to different branchlets within the same primary subtree was very similar to that seen for inputs delivered to entirely different subtrees—near-linear summation over most of the stimulus range with a slight amplification for very large inputs (Fig. 5f,g). Similar results were obtained in four additional neurons.

The strong effect of spatial separation of two inputs within a branch indicates that the basic integrative compartment in thin dendrites for paired-pulse stimuli may be a sliding window of a few tens of microns in (unbranched) length. The boundaries of the nonlinear interaction zone are evidently soft, however, in that superlinear summation can occur at greater separations, albeit in an attenuated form, and/or can span a branch point, when the inputs are made very strong.

## DISCUSSION

We tested the rules of subthreshold synaptic summation under varying conditions of interelectrode spacing and ISI, both within and between the thin-branch basal and apical oblique subtrees of layer-5 neocortical pyramidal neurons. Overall, our findings allow us to reject the hypothesis that the thin basal and apical oblique dendrites of layer-5 neocortical pyramidal neurons function as global summing units that are either linear or are subject to any single output nonlinearity. Rather, our findings support the two-layer sum-of-subunits model<sup>31</sup> to the extent that (i) a local sigmoidal thresholding nonlinearity modulates summation within each dendritic compartment, and (ii) the outputs of different compartments sum linearly at the cell body. Our observation of two-layer summation behavior in thin den-

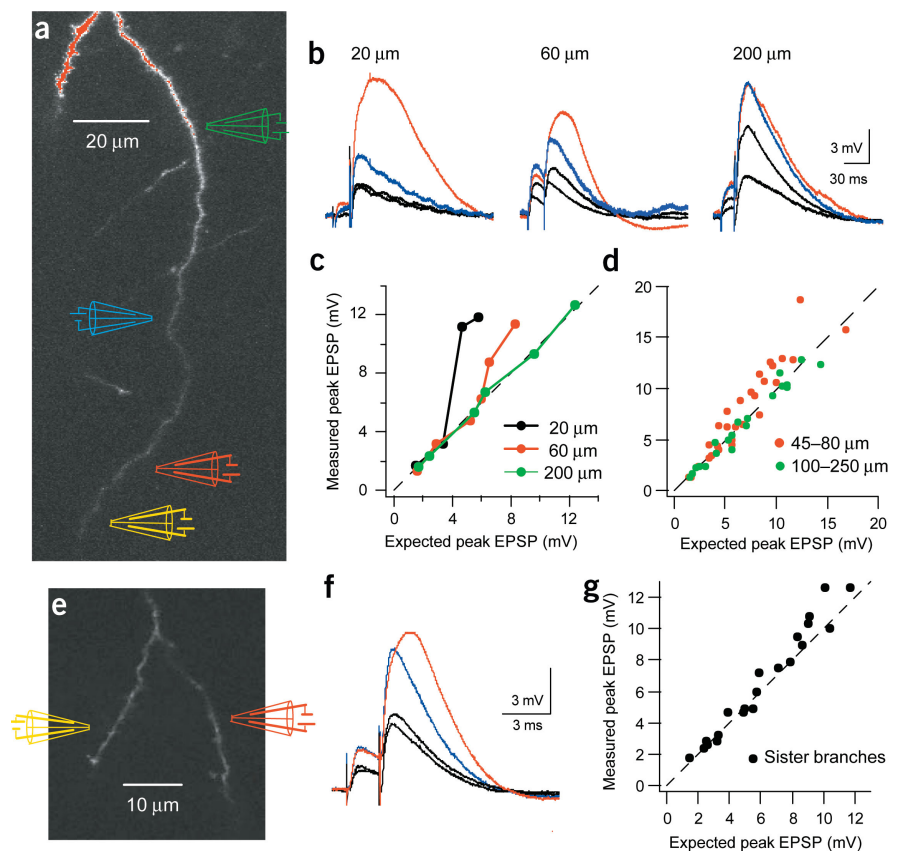


**Figure 5** Defining the size of the nonlinear integration compartment. (a) A single basal branch was stimulated with two electrodes with interelectrode spacings of 20–200  $\mu\text{m}$ . Electrode position is shown schematically, with the yellow electrode acting as a fixed reference point. (b) Example traces show summation of EPSPs at three interelectrode distances (color scheme for traces as in Figs. 2 and 3). The voltage traces are averages of four individual sweeps. (c) Expected versus actual somatic EPSPs are shown for a range of stimulus intensities at three different electrode spacings. (d) Summary plot ( $n = 9$ ) showing expected versus actual somatic EPSPs for two interelectrode spacings (45–80  $\mu\text{m}$  in red, >100  $\mu\text{m}$  in green). Modest superlinearity can occur for interelectrode spacings of 45–80  $\mu\text{m}$  but are not seen for larger spacings. (e) Electrodes were positioned on sister branches ~20  $\mu\text{m}$  from a distal basal branch point (interelectrode distance of ~40  $\mu\text{m}$ ). (f) Example traces show slight superlinearity for very strong inputs. (g) Expected versus actual somatic EPSPs are shown for two inputs separated by a branch point, at a range of stimulus intensities ( $n = 5$ ). Overall, summation is essentially linear. Slight superlinearity, as in f, occurs only at high stimulus intensities.

drites of pyramidal neurons, which has not previously been reported, was facilitated by several factors including (i) our ability to precisely localize the sites of synaptic excitation through calcium imaging; (ii) the use of paired-pulse rather than single-pulse stimuli, which were more effective at evoking local regenerative currents; (iii) the use of systematically varying stimulus intensity in multiple experiments on the same dendritic branch; (iv) manipulation of interelectrode distance within the same branch and (v) controlled comparisons of within-branch versus between-branch summation. In the present experiments, we did not pursue in detail the channel mechanisms underlying the sigmoidal thresholding nonlinearity governing within-branch integration. Nevertheless, the shape, amplitude and NMDA dependence of this response indicate that the sigmoidal behavior may be mediated by NMDA spikes, as previously described in basal dendrites of pyramidal neurons<sup>28</sup>.

It is important to specify that our results pertain to the arithmetic of subthreshold synaptic integration in pyramidal neurons and could change in either minor or substantive ways when stimu-

lus conditions are strong enough to drive full-blown axosomatic spiking. Furthermore, we have so far studied within-branch summation for only a single branch at a time, and between-branch summation using only pairs of branches. Additional experiments will be needed to determine whether the two-layer model continues to predict responses of pyramidal neurons in the more realistic suprathreshold case and when stimuli are delivered to multiple branches simultaneously. A recent compartmental modeling study provides grounds for optimism<sup>32</sup>.

Our results focus on summation within and between thin basal and apical oblique dendrites, and they support a two-layer model of synaptic integration in these portions of the cell. The two-layer model is different from, but not incompatible with, the more commonly discussed two-compartment view of the pyramidal neuron. Unlike the two-layer model, whose first layer consists of several dozen separately thresholded thin-branch subunits, the two-compartment view refers to two main integrative subregions of the cell: a proximal region, including the basal dendrites, soma and apical obliques, and a distal region consisting of the apical tuft. The two-compartment view has proven most useful in guiding experiments involving interactions between the slow calcium-spiking mechanisms in the distal compartment and the fast sodium-spiking mechanism at the cell body<sup>15,18,34</sup>. We consider it possible that the two-layer and two-compartment views of the pyramidal neuron may ultimately be merged. According to this view, the distal apical compartment may function as a separate two-layer network whose output, which is mediated by the apical calcium spike generator, interacts multiplicatively with the proximal two-layer network—in effect leading to a three-layer model (see Figure 3 in ref. 15).

One important difference between the two-layer sum-of-subunits model<sup>31</sup> and the data presented here pertains to the degree of within-branch compartmentalization. At odds with the one-to-one mapping between thin terminal branches and dendritic subunits that was previously proposed<sup>31,32</sup>, our results suggest a more subtle compartmentalization scheme in which interstimulus distance and intervening branch points modulate the degree to which two inputs interact under the same local compartment nonlinearity. This type of sliding interaction zone was incorporated in an earlier single-neuron abstraction called the clusteron<sup>35</sup>, which was functionally equivalent to a two-layer model whose first layer contains a large number of virtual subunits with overlapping inputs. The clusteron model was designed in part to demonstrate how a Hebbian learning rule, combined with structural plasticity at the interface between axons and dendrites, can lead similarly activated synapses to aggregate within the same postsynaptic dendritic compartment<sup>36</sup>. Although potentially providing greater processing power than the one-nonlinearity-per-branch scheme (this remains an open question), neurons with sliding subunits are more complicated to analyze mathematically and to study experimentally. *In vivo*, the size of the integrative subunits of a cell and their degree of overlap within a branch could also depend on the density and distribution of excitatory input that is delivered to the branch, the effects of local inhibition and the rate of somatic spiking. The consequences for synaptic integration of each of these influences are as yet unknown. Given that the computational power of a neuron grows roughly in proportion to the number of independent nonlinear subunits it can support<sup>15,37–39</sup>, the two-layer view of the pyramidal cell could have broad implications for the information processing<sup>40,41</sup> and memory-related functions of cortical tissue<sup>36</sup>. It is also worth noting that neuronal computations involving multiple dendritic subunits have been described in other neural systems, including starburst amacrine cells in the rabbit retina<sup>42,43</sup> and

*Drosophila melanogaster* visual interneurons<sup>44</sup>. Future experiments will be needed to determine whether functional input clustering occurs in thin branches of pyramidal neurons as well, and to what extent synaptically evoked dendritic spikes regularly occur and are involved in the moment-to-moment operation of the living brain.

## METHODS

**Slice preparation and electrophysiological recording.** Neocortical brain slices that were 300–350  $\mu\text{m}$  thick were prepared from 18- to 28-day-old Wistar rats. Whole-cell patch-clamp recordings were made from visually identified layer-5 pyramidal neurons using infrared-differential interference contrast optics. The extracellular solution contained 125 mM NaCl, 25 mM  $\text{NaHCO}_3$ , 25 mM glucose, 3 mM KCl, 1.25 mM  $\text{NaH}_2\text{PO}_4$ , 2 mM  $\text{CaCl}_2$  and 1 mM  $\text{MgCl}_2$  (pH 7.4) at 35–36 °C. The intracellular solution contained 115 mM  $\text{K}^+$ -gluconate, 20 mM KCl, 2 mM Mg-ATP, 2 mM  $\text{Na}_2$ -ATP, 10 mM  $\text{Na}_2$ -phosphocreatine, 0.3 mM GTP, 10 mM HEPES and 0.15 mM Calcium Green-1 (CG-1) or 0.2 mM Oregon Green 488 Bapta-1 (OGB-1), pH 7.2. Bicuculline methiodide (BCC; 1–20  $\mu\text{M}$ ) was added to the extracellular solution in some experiments. The electrophysiological recordings were performed using Multi-Clamp 700A (Axon Instruments), and the data were acquired and analyzed using Pclamp 8.2 (Axon Instruments) and in-house and Igor (Wavemetrics) software. All statistical analyses used the Student's *t*-test.

**Focal synaptic stimulation and calcium fluorescence imaging.** Focal synaptic stimulation was performed with a theta patch pipette located in close proximity to the selected basal dendritic segment, as guided by the fluorescent image of the dendrite. We limited ourselves to dendritic regions that were more distal than the initial 50- $\mu\text{m}$  segment of the basal dendrites, as we could not obtain focal synaptic activation in those regions. The neurons were filled with a calcium-sensitive dye (CG-1 or OGB-1) and the basal dendritic tree was imaged with a confocal imaging system (Olympus Fluoview) mounted on an upright BX51WI Olympus microscope equipped with a 60 $\times$  (0.9 n.a.; Olympus) water objective. The theta stimulating electrodes were filled with Alexa Fluor 647. Full images were obtained with a temporal resolution of 1 Hz and in the line scan mode with a temporal resolution of 512 Hz. Images were analyzed using Tiempo (Olympus) and in-house and Igor software.

## ACKNOWLEDGMENTS

We thank M. Hausser, M. London and Y. Schiller for their helpful comments on an earlier version of the manuscript. This study was supported by the National Institutes of Health, Israeli Science Foundation, National Science Foundation and the Rappaport Foundation.

## COMPETING INTERESTS STATEMENT

The authors declare that they have no competing financial interests.

Received 26 January; accepted 15 April 2004

Published online at <http://www.nature.com/natureneuroscience/>

1. Hausser, M., Spruston, N. & Stuart, G.J. Diversity and dynamics of dendritic signaling. *Science* **290**, 739–744 (2000).
2. Magee, J., Hoffman, D., Colbert, C. & Johnston, D. Electrical and calcium signaling in dendrites of hippocampal pyramidal neurons. *Annu. Rev. Physiol.* **60**, 327–346 (1998).
3. Rhodes, P.A. Functional implications of active currents in the dendrites of pyramidal neurons. in *Cerebral Cortex Vol. 13* (eds. Ullinski, P.S., Jones, E.G. & Peters, A.) 139–200 (Kluwer Academic Press, New York, 1999).
4. Reyes, A. Influence of dendritic conductances on the input-output properties of neurons. *Annu. Rev. Neurosci.* **24**, 653–675 (2001).
5. Schiller, J. & Schiller, Y. NMDA receptor-mediated dendritic spikes and coincident signal amplification. *Curr. Opin. Neurobiol.* **11**, 343–348 (2001).
6. Migliore, M. & Shepherd, G.M. Emerging rules for the distributions of active dendritic conductances. *Nat. Rev. Neurosci.* **3**, 362–370 (2002).
7. Johnston, D., Magee, J., Colbert, C. & Christie, B.R. Active properties of neuronal dendrites. *Annu. Rev. Neurosci.* **19**, 165–186 (1996).
8. Margulis, M. & Tang, C.M. Temporal integration can readily switch between sublinear and supralinear summation. *J. Neurophysiol.* **79**, 2809–2813 (1998).
9. Urban, N.N. & Barrionuevo, G. Active summation of excitatory postsynaptic potentials in hippocampal CA3 pyramidal neurons. *Proc. Natl. Acad. Sci. USA* **95**, 11450–11455 (1998).
10. Cash, S. & Yuste, R. Linear summation of excitatory inputs by CA1 pyramidal neurons. *Neuron* **22**, 383–394 (1999).

11. Magee, J.C. Dendritic integration of excitatory synaptic input. *Nat. Rev. Neurosci.* **1**, 181–190 (2000).
12. Nettleton, J.S. & Spain, W.J. Linear to supralinear summation of AMPA-mediated EPSPs in neocortical pyramidal neurons. *J. Neurophysiol.* **83**, 3310–3322 (2000).
13. Oakley, J.C., Schwandt, P.C. & Crill, W.E. Dendritic calcium spikes in layer 5 pyramidal neurons amplify and limit transmission of ligand-gated dendritic current to soma. *J. Neurophysiol.* **86**, 503–513 (2001).
14. Tamas, G., Szabadics, J. & Somogyi, P. Cell type- and subcellular position dependent summation of unitary postsynaptic potentials in neocortical neurons. *J. Neurosci.* **22**, 740–747 (2002).
15. Häusser, M. & Mel, B.W. Dendrites: bug or feature. *Curr. Opin. Neurobiol.* **13**, 372–383 (2003).
16. Cauller, L.J. & Connors, B.W. Synaptic physiology of horizontal afferents to layer I in slices of rat SI neocortex. *J. Neurosci.* **14**, 751–762 (1994).
17. Schiller, J., Schiller, Y., Stuart, G. & Sakmann, B. Calcium action potentials restricted to distal apical dendrites of rat neocortical pyramidal neurons. *J. Physiol.* **505**, 605–616 (1997).
18. Larkum, M.E., Zhu, J.J. & Sakmann, B. A new cellular mechanism for coupling inputs arriving at different cortical layers. *Nature* **398**, 338–341 (1999).
19. Oviedo, H. & Reyes, A.D. Boosting of neuronal firing evoked with asynchronous and synchronous inputs in the dendrite. *Nat. Neurosci.* **5**, 261–266 (2002).
20. Williams, S.R. & Stuart, G.J. Dependence of EPSP efficacy on synapse location in neocortical pyramidal neurons. *Science* **295**, 1907–1910 (2002).
21. Bernander, O., Koch, C. & Douglas, R.J. Amplification and linearization of distal synaptic input to cortical pyramidal cells. *J. Neurophysiol.* **70**, 2743–2753 (1994).
22. Cook, E.P. & Johnston, D. Voltage-dependent properties of dendrites that eliminate location-dependent variability of synaptic input. *J. Neurophysiol.* **81**, 535–543 (1999).
23. Magee, J.C. Dendritic Ih normalizes temporal summation in hippocampal CA1 neurons. *Nat. Neurosci.* **2**, 508–514 (1999).
24. Magee, J.C. & Cook, E.P. Somatic EPSP amplitude is independent of synapse location in hippocampal pyramidal neurons. *Nat. Neurosci.* **3**, 895–903 (2000).
25. Larkman, A.U. Dendritic morphology of pyramidal neurons of the rat: spine distribution. *J. Comp. Neurol.* **306**, 332–343 (1991).
26. Megias, M., Emri, Z., Freund, T.F. & Gulyas, A.I. Total number and distribution of inhibitory and excitatory synapses on hippocampal CA1 pyramidal cells. *Neuroscience* **102**, 527–540 (2001).
27. Beaulieu, C. & Colonnier, M. A laminar analysis of the number of round-asymmetrical and flat-symmetrical synapses on spines, dendritic trunks, and cell bodies in area 17 of the cat. *J. Comp. Neurol.* **231**, 180–189 (1985).
28. Schiller, J., Major, G., Koester, H.J. & Schiller, Y. NMDA spikes in basal dendrites of cortical pyramidal neurons. *Nature* **404**, 285–289 (2000).
29. Wei, D.-S. *et al.* Compartmentalized and binary behavior of terminal dendrites in hippocampal pyramidal neurons. *Science* **293**, 2272–2275 (2001).
30. Ariav, G., Polsky, A. & Schiller, J. Submillisecond precision of the input-output information function mediated by fast sodium dendritic spikes in basal dendrites of CA1 pyramidal neurons. *J. Neurosci.* **23**, 7750–7758 (2003).
31. Poirazi, P., Brannon, T. & Mel, B.W. Arithmetic of subthreshold synaptic summation in a model CA1 pyramidal cell. *Neuron* **37**, 977–987 (2003).
32. Poirazi, P., Brannon, T. & Mel, B.W. Pyramidal neuron as two-layer network. *Neuron* **37**, 989–999 (2003).
33. McClelland, J.L. & Rumelhart, D.E. Distribution memory and the representation of general and specific information. *J. Exp. Psychol. Gen.* **114**, 159–197 (1985).
34. Kepecs, A., Wang, X.J. & Lisman, J. Bursting neurons signal input slope. *J. Neurosci.* **22**, 9053–9062 (2002).
35. Mel, B.W. The clusteron: toward a simple abstraction for a complex neuron. in *Advances in Neural Information Processing Systems, Vol. 4* (eds. Moody, J., Hanson, S. & Lippmann, R.) 35–42 (Morgan Kaufmann, San Mateo, CA, 1992).
36. Poirazi, P. & Mel, B.W. Impact of active dendrites and structural plasticity on the memory capacity of neural tissue. *Neuron* **29**, 779–796 (2001).
37. Koch, C., Poggio, T. & Torre, V. Nonlinear interaction in a dendritic tree: localization, timing and role of information processing. *Proc. Natl. Acad. Sci. USA* **80**, 2799–2802 (1983).
38. Rall, W. & Segev, I. Functional possibilities for synapses on dendrites and on dendritic spines. in *Synaptic Function* (eds. Edelman, G., Gall, W. & Cowan, W.) 605–636 (Wiley, New York, 1987).
39. Shepherd, G.M. & Brayton, R. Logic operations are properties of computer-simulated interactions between excitable dendritic spines. *Neuroscience* **21**, 151–165 (1987).
40. Archie, K.A. & Mel, B.W. An intradendritic model for computation of binocular disparity. *Nat. Neurosci.* **3**, 54–63 (2000).
41. Mel, B.W., Ruderman, D.L. & Archie, K.A. Translation-invariant orientation tuning in visual 'complex' cells could derive from intradendritic computations. *J. Neurosci.* **18**, 4325–4334 (1998).
42. Euler, T., Detwiler, P.B. & Denk, W. Directionally selective calcium signals in dendrites of starburst amacrine cells. *Nature* **418**, 845–852 (2002).
43. Borg-Graham, L.J. & Grzywacz, N. A model of the direction selectivity circuit in retina: transformations by neurons singly and in concert. in *Single Neuron Computation* (eds. McKenna, T., Davis, J. & Zornetzer, S.F.) 347–375 (Academic Press, Cambridge, Massachusetts, 1992).
44. Single, S. & Borst, A. Dendritic integration and its role in computing image velocity. *Science* **281**, 1848–1850 (1998).